Impact of extreme ultraviolet radiation on the scintillation of pure and xenon-doped liquid argon

LIDINE 2025 Hong Kong

Evangelia Nikoloudaki on behalf of the X-ArT collaboration



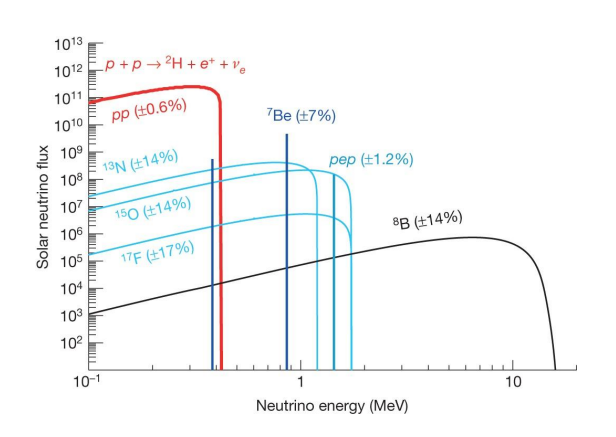


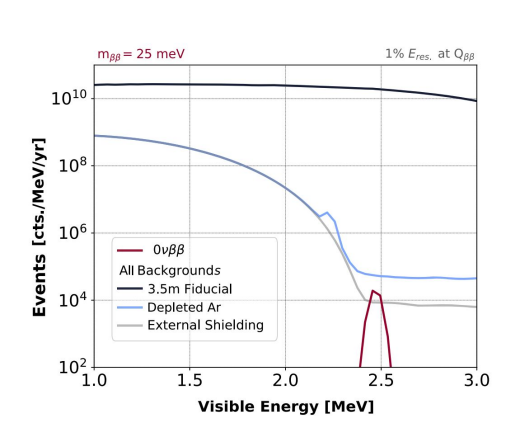


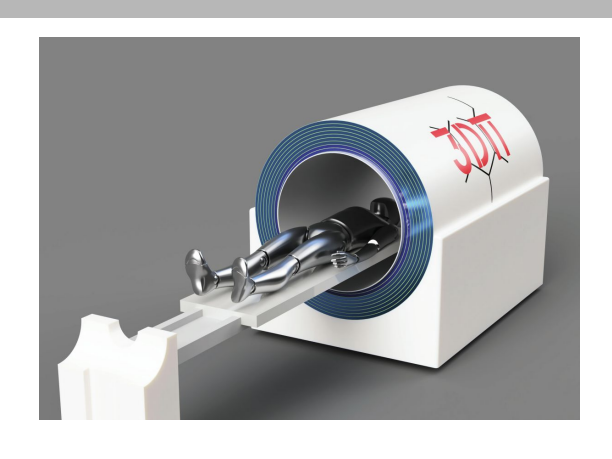


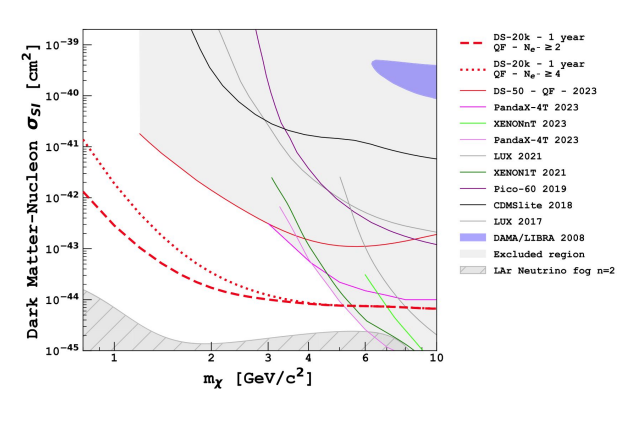
Xenon doped liquid argon

- faster scintillation: sub-nanosecond timing resolution
- higher photon and ionization yield
- longer photon attenuation length
- lower energy thresholds
- cost effective
- argon boiling temperature









X-ArT: Xenon-Argon Technology

- 1. Study the **thermodynamic** properties:
 - a. Ar-Xe phase diagram
 - b. Maximum Xe solubility in LAr
- 2. Characterize the Ar-Xe response in scintillation and ionization up to the maximum Xe solubility
 - a. phase 1: scintillation only up to 40 ppm of xenon concentration
 - b. phase 2: ionization up to maximum solubility

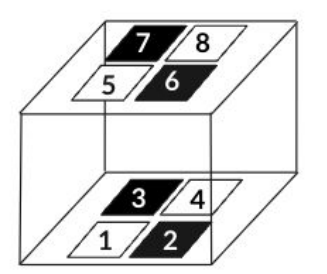


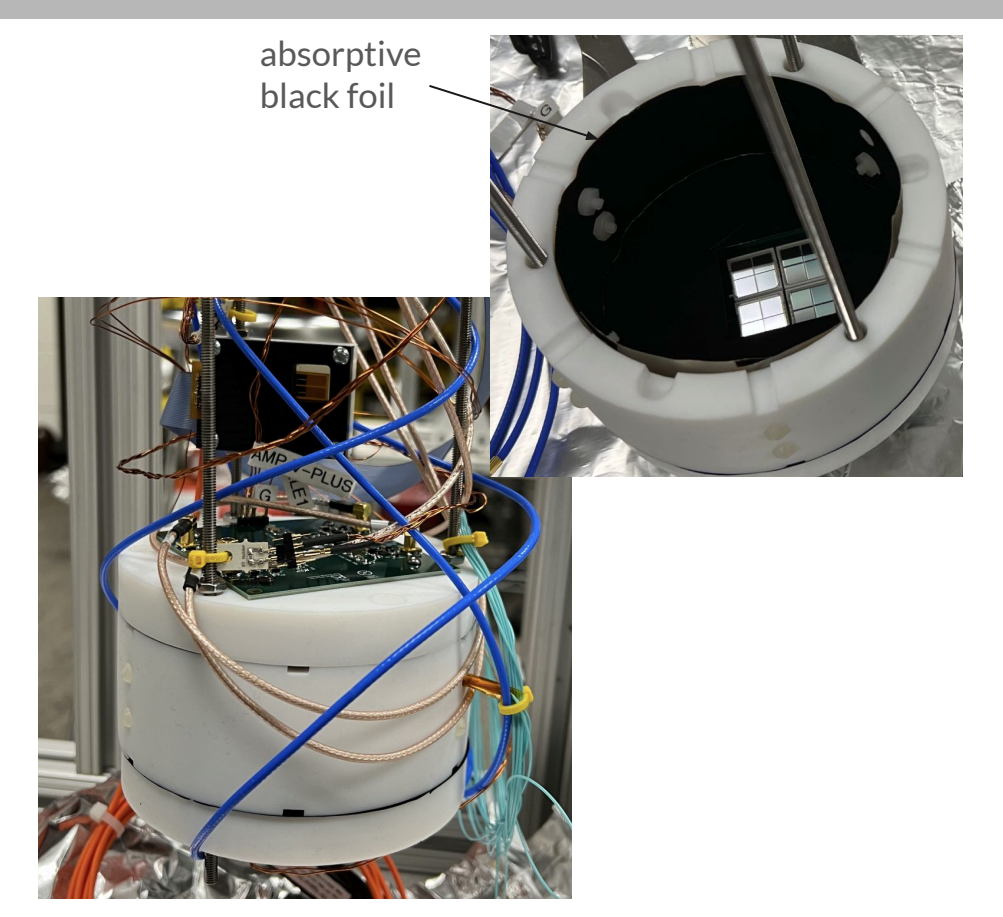
Experimental setup at Princeton

PHYSICAL REVIEW D 111 102001 (2024)

Single phase LAr cylindrical chamber

- 4.5 cm height / 9.5 cm diameter
- no TPB wavelength shifter
- black foil to prevent reflections
- 32 VUV-sensitive Hamamatsu S13371 SiPMs
 - 4 SiPMs per channel (8 channels)
 - 4 channels with quartz window (WW)
 - 4 channels without window (WL)





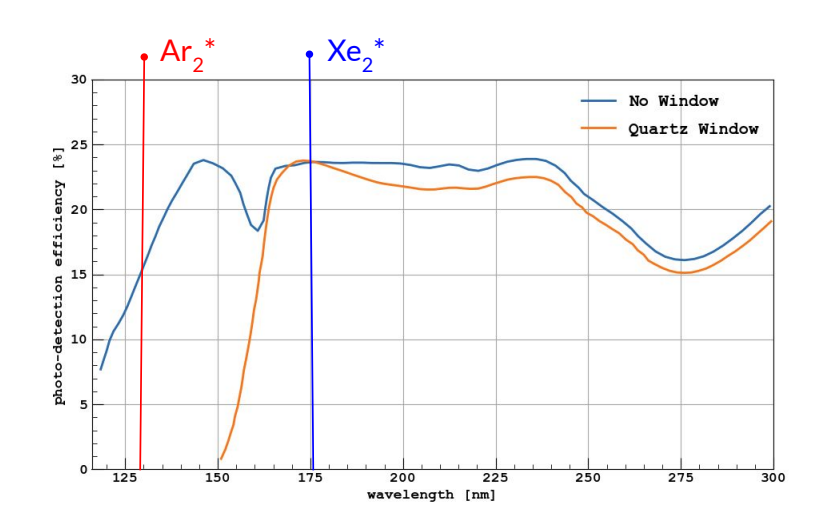
Detection channels

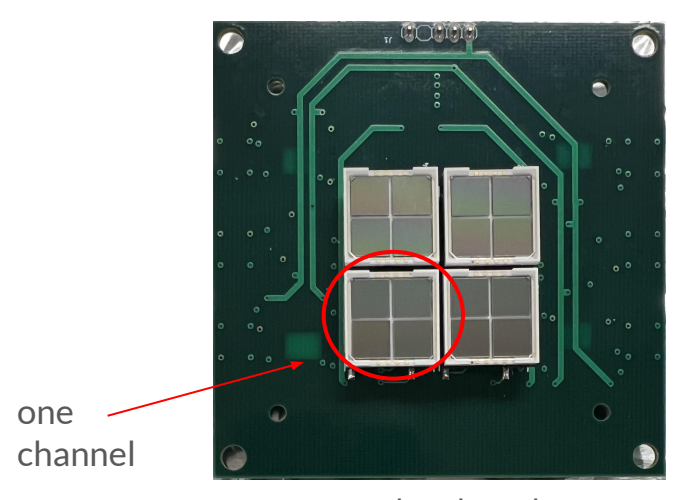
WW channels: sensitive above ~150 nm

→ detect only Xe₂* photons (175 nm)

WL channels: sensitive above ~60 nm

 \rightarrow detect both Xe₂* (175 nm) and Ar₂* (128 nm) photons





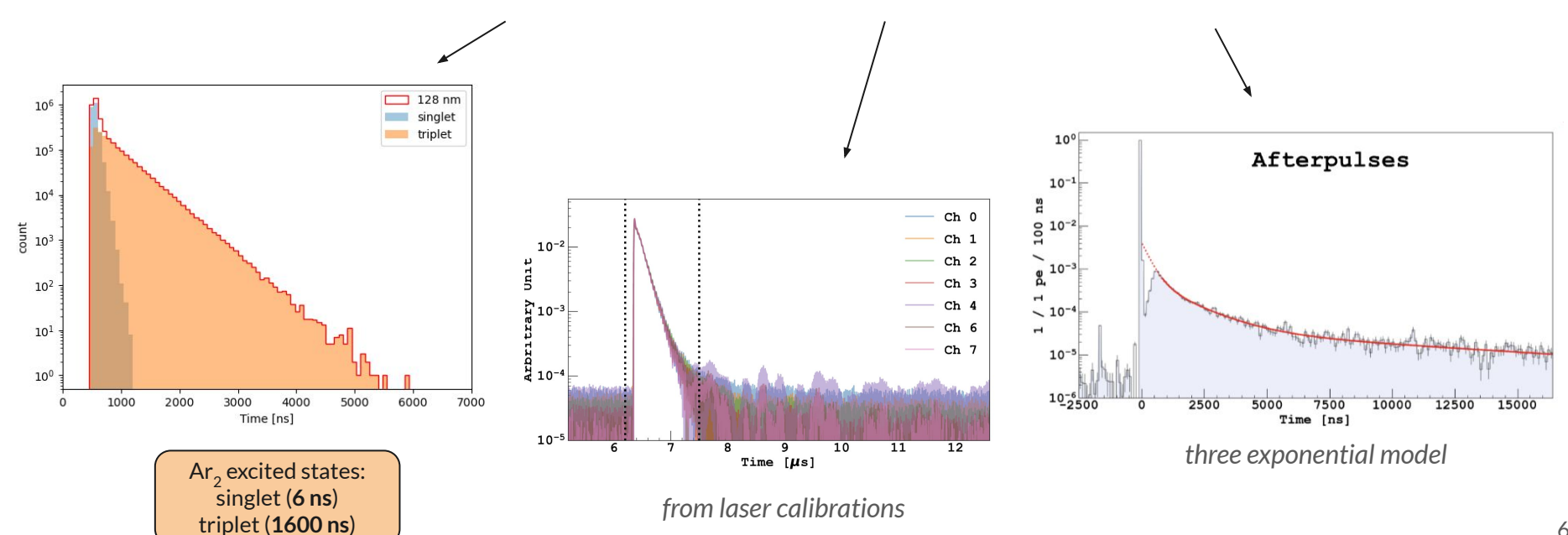
readout board

Characterization of the LAr response

Pure LAr measurement (WL-SiPMs only) to constrain the Ar_2^* triplet lifetime and characterize the LAr purity.

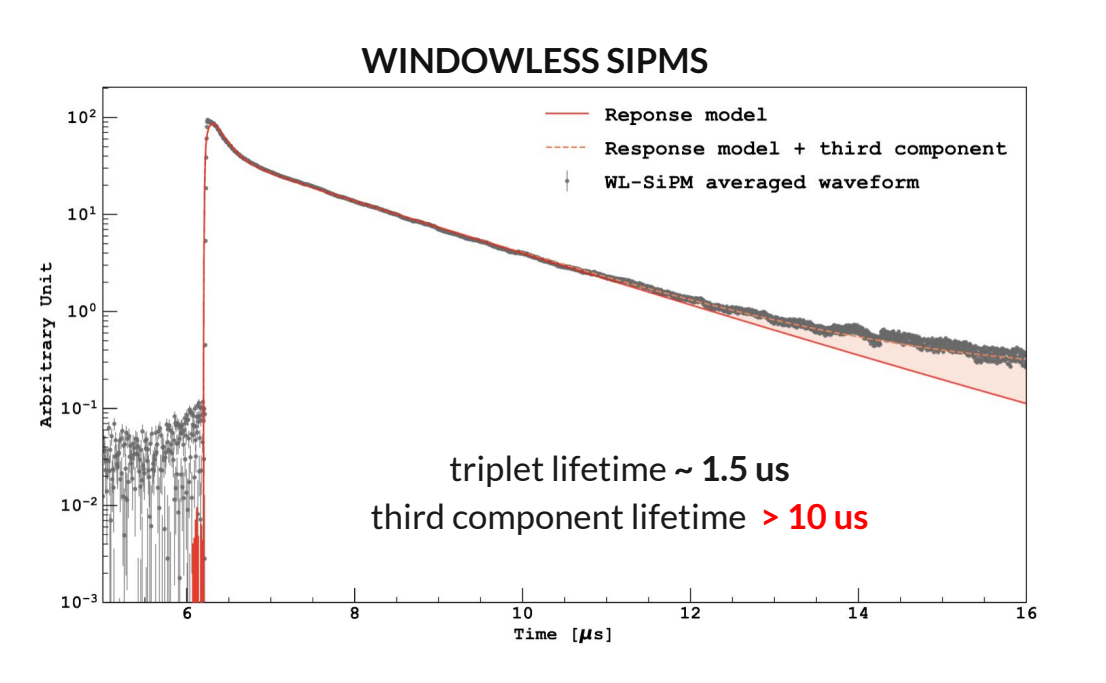
LAr scintillation response model:

sum of singlet and triplet state exponentials \otimes SiPM time response \otimes SiPM AP time profile



Characterization of the LAr response

Long component observed with WL-SiPMs:



In literature it is assigned to:

- TPB fluorescence
- Teflon fluorescence
- Near-infrared photons (> 800 nm)

TPB fluorescence ? \rightarrow NO

o no TBP in the X-ArT setup

Teflon fluorescence? → NO

all teflon components covered with black foil

Near-infrared photons? → NO

detected at < 150 nm

Afterpulses ? \rightarrow NO

APs only cannot explain the long tail

EUV emission in LAr

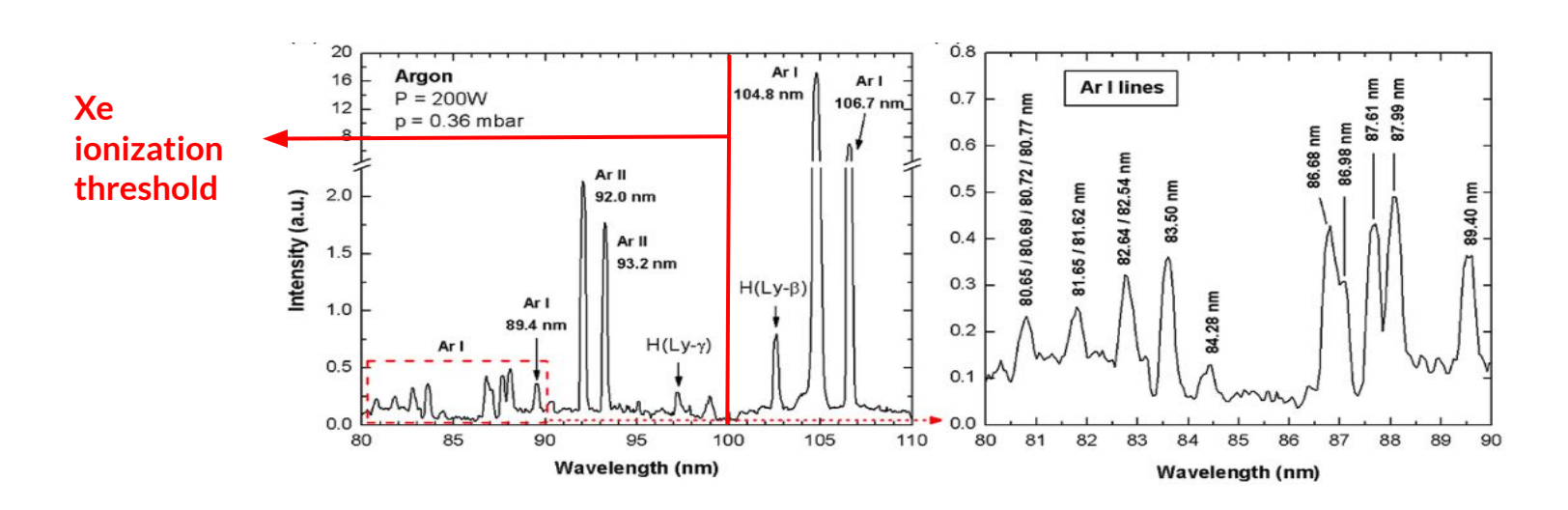
Ar-I: neutral argon (Ar*)

Ar-II: singly or multiple ionized argon (Ar^{q+})

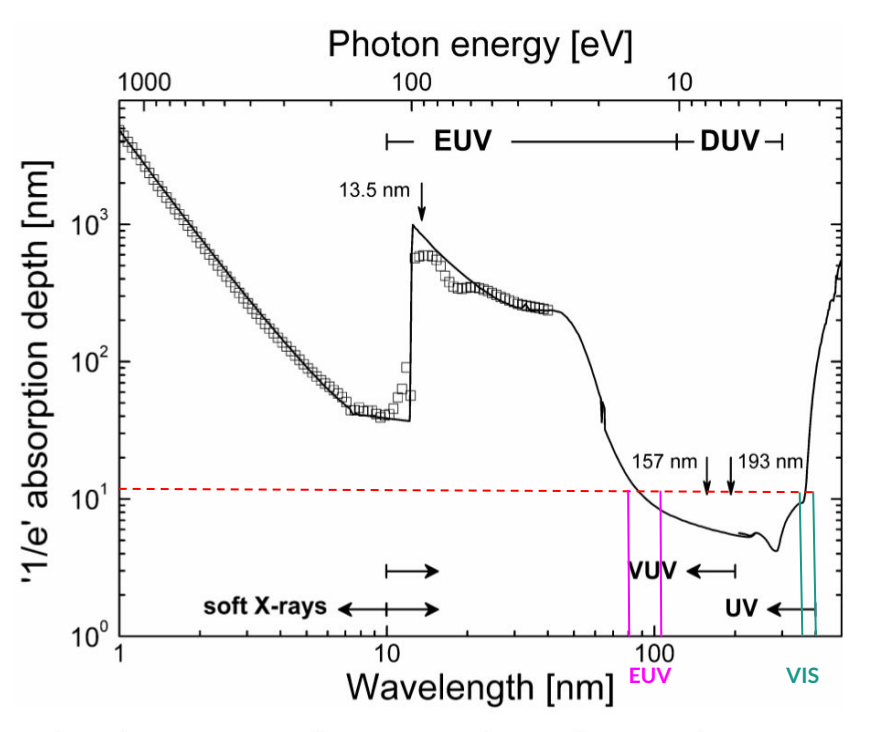
EUV range: ~10-100 nm

Emission from metastable states: ms to s

- 1. It is well known from atomic physics that Ar-I and Ar-II emit EUV photons from metastable levels.
- 2. EUV photons with wavelength < 100 nm or energy > 12.1 eV can ionize Xe atoms.



EUV detectable with SiPMs? → **YES**



EUV and VIS have almost the same absorption length in silicon.

Fig. 7. '1/e' absorption depth in Si as a function of incident radiation wavelength (Palik, 1985; Henke data).

EUV detectable with TPB/PMTs? → **YES**

Eur. Phys. J. C (2018) 78:329

TPB is efficient at EUV.

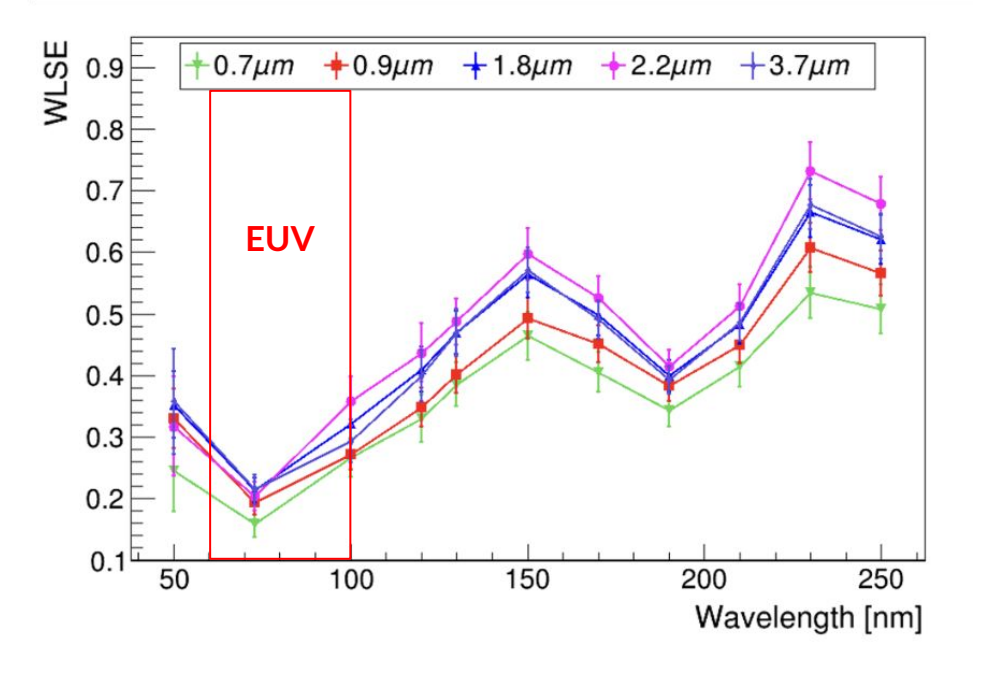
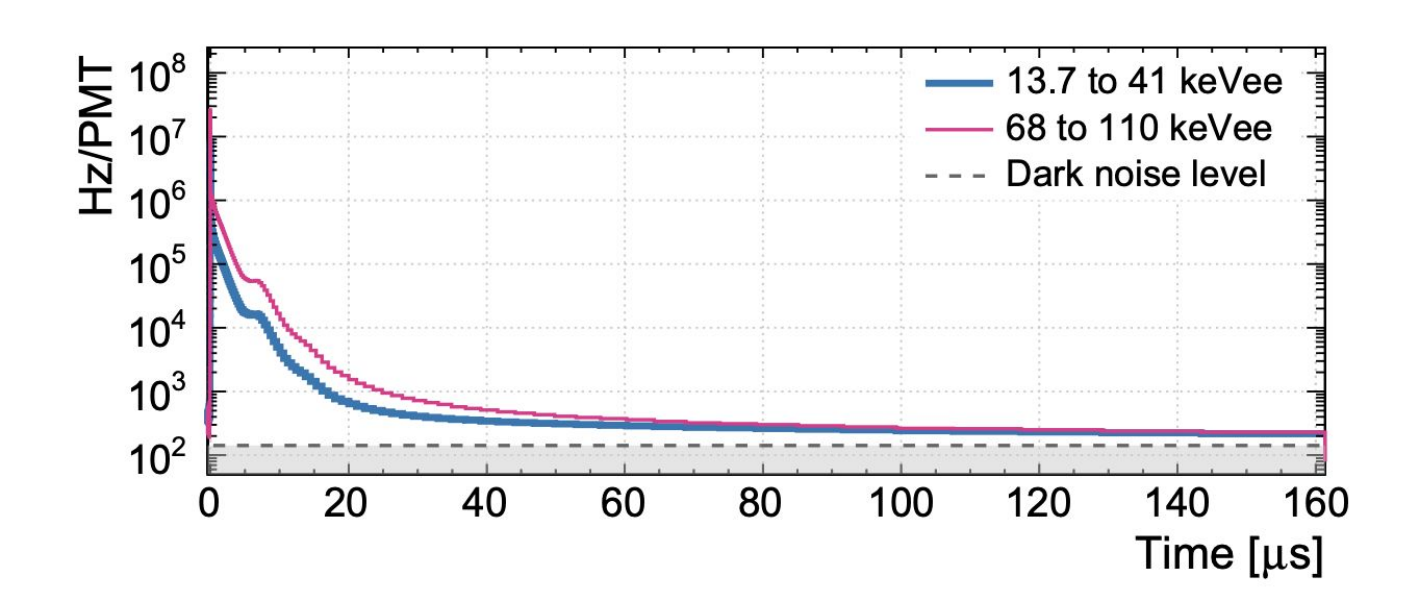


Fig. 16 Absolute WLSE efficiency for several samples of various thickness

Long component in DEAP-3600

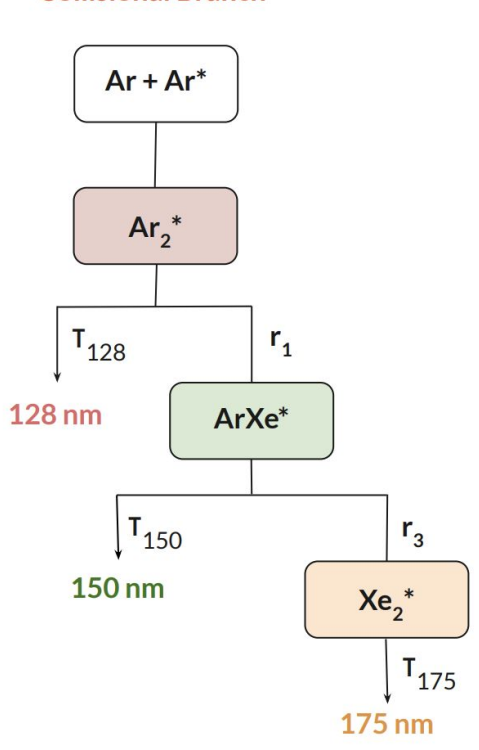
DEAP-3600:

- **liquid argon** detector for dark matter searches
- uses TPB wavelength shifter (UV to VIS conversion) and PMTs to detect the scintillation light

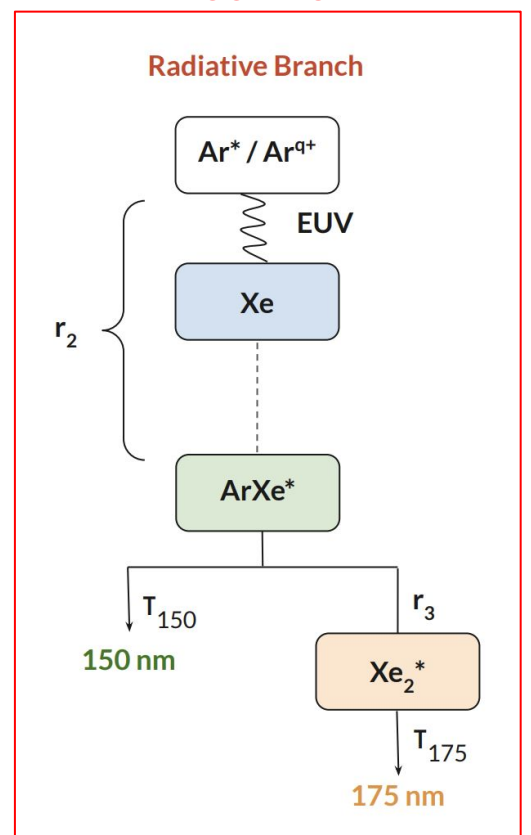


The Xe-Ar scintillation model

Collisional Branch



NEW COMPONENT



 $r_1 \rightarrow \text{ rate of } ArXe^* \text{ formation}$

r₂ → rate of **EUV-induced** ionization and subsequent **ArXe*** formation

 $r_3 \rightarrow \text{ rate of } Xe_2^* \text{ formation}$

Two competitions between:

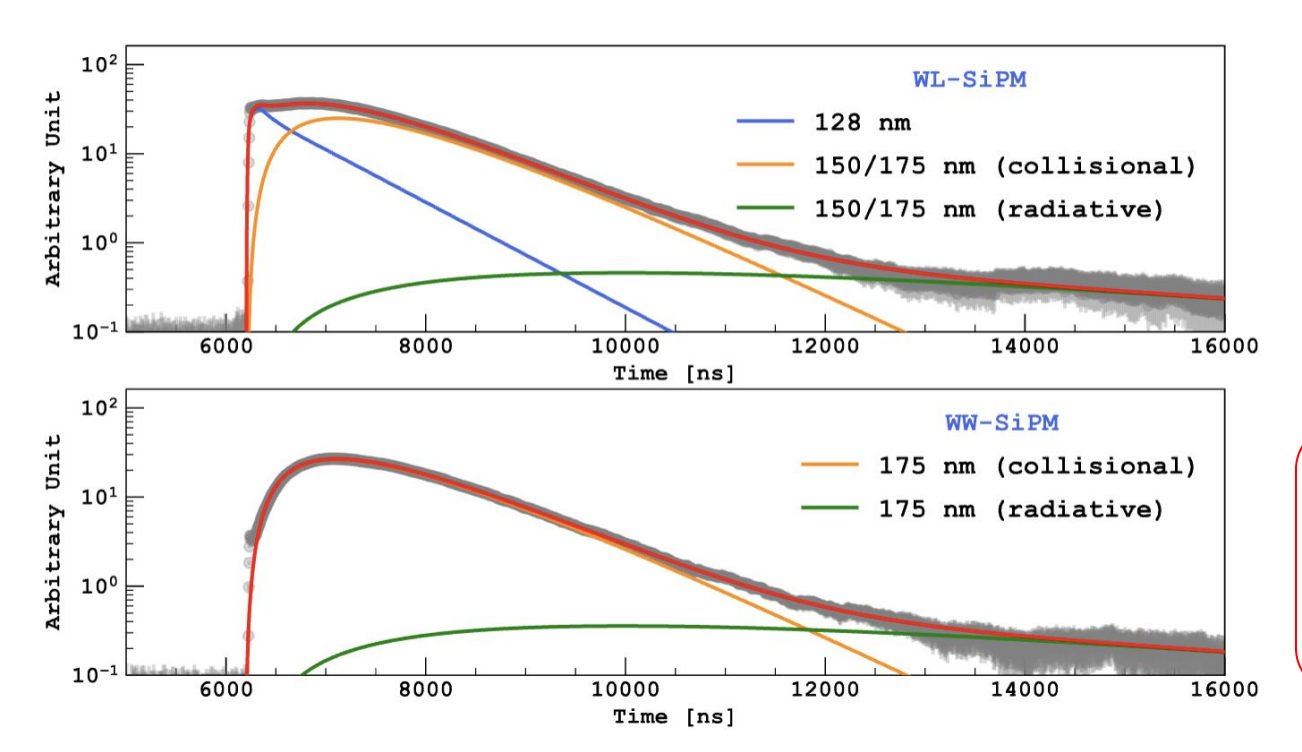
- triplet decay and ArXe* formation
- ArXe* de-excitation and Xe_2^* formation

The analytical model

.3

Simultaneous fit of WL- and WW-SiPM waveforms

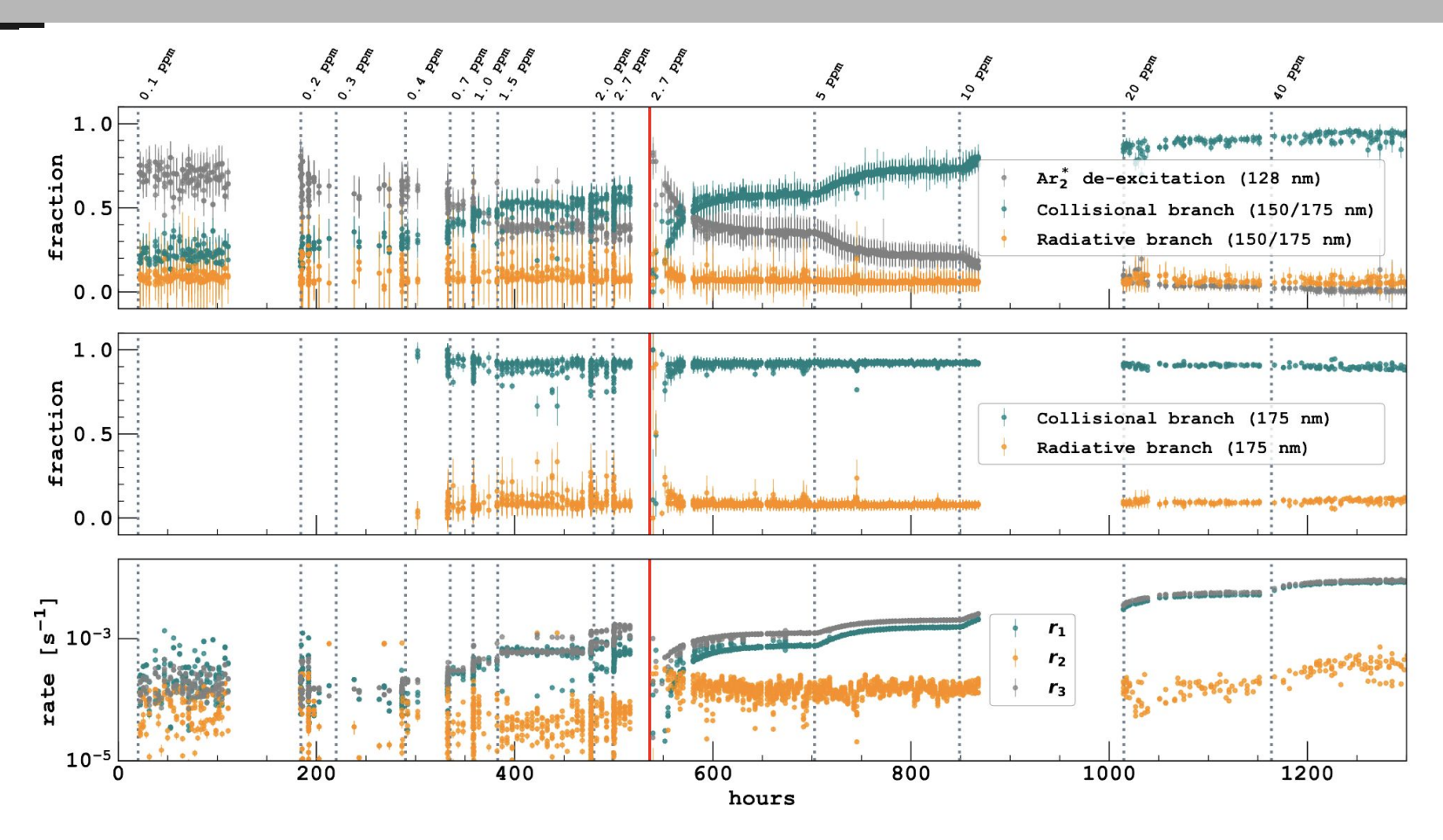
2.7 ppm of Xe and ⁶⁰Co source



rate parameters (r_1 , r_2 , and r_3) are constrained between the two fits

- Non-zero contribution from the radiative process.
- The collisional process alone, cannot explain the data.

Effects of the Xe concentration



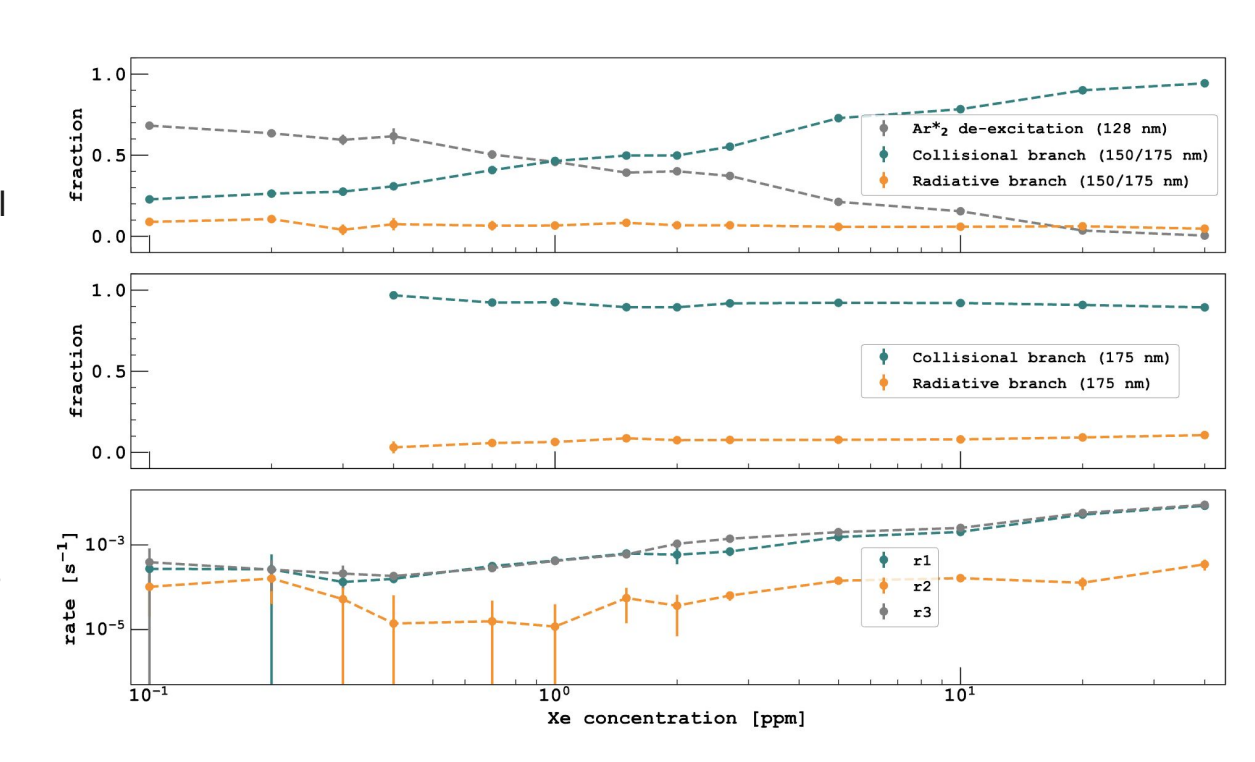
Effects of the Xe concentration

Collisional branch increase with Xe:

 increasing probability of collisional energy transfer

Radiative branch is constant:

- o depends on atomic Ar excitation
- mean EUV Xe scattering length is negligible with respect to the chamber size

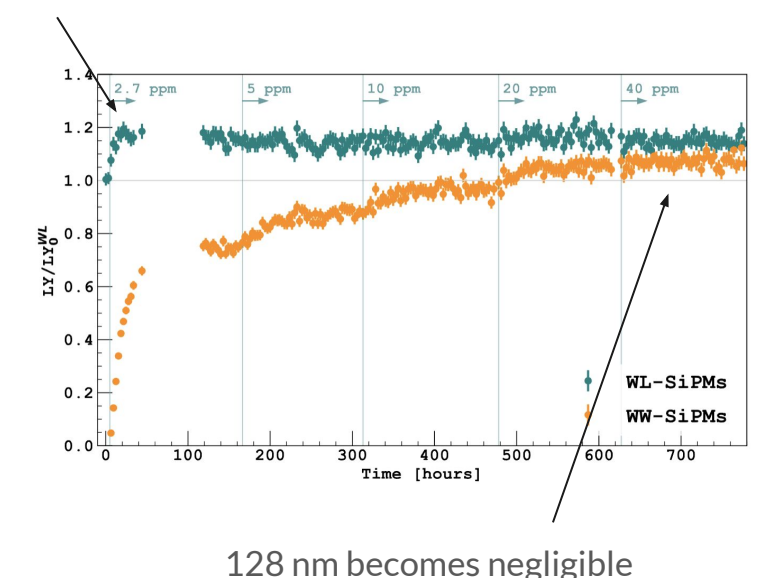


Xe-doped liquid argon light yield and PSD

LY increases with increasing Xe concentration.

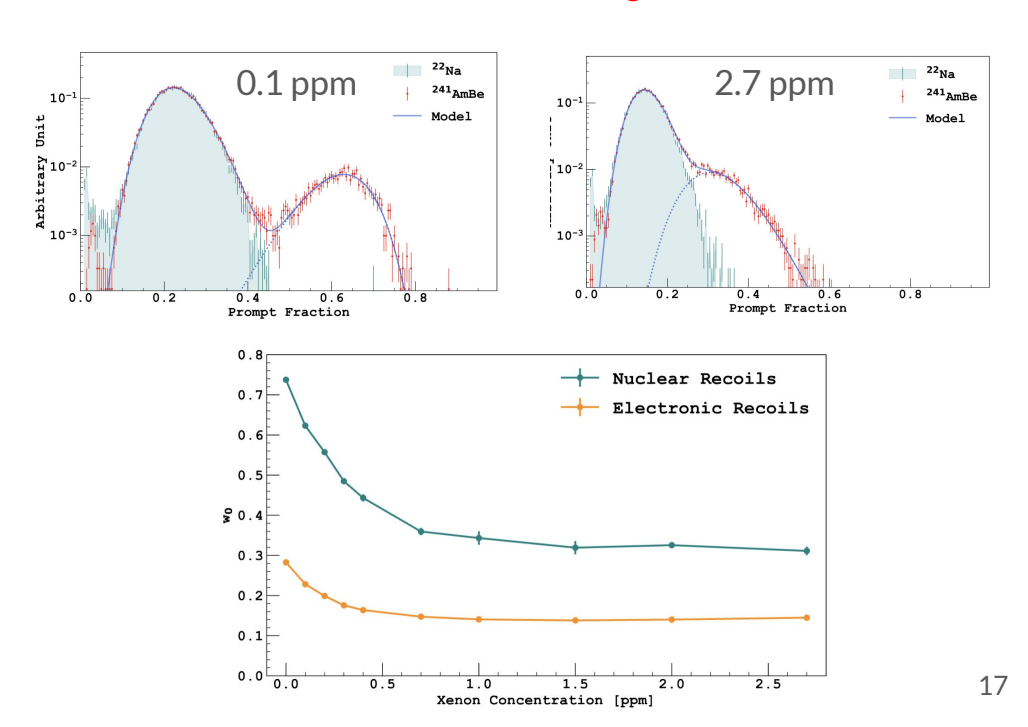
overall LY = sum of Ar_2^* , Xe_2^* and $ArXe^*$ photons

increase due to the radiative component



PSD degrades with increasing Xe concentration.

PSD observable w: the fraction of light in the first 300 ns



EUV as natural source of spurious electrons

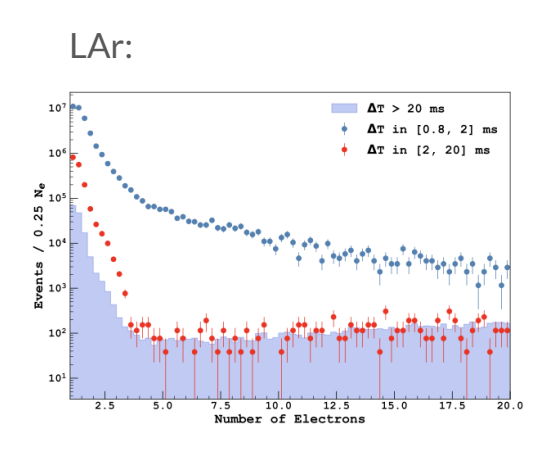
Spurious electrons:

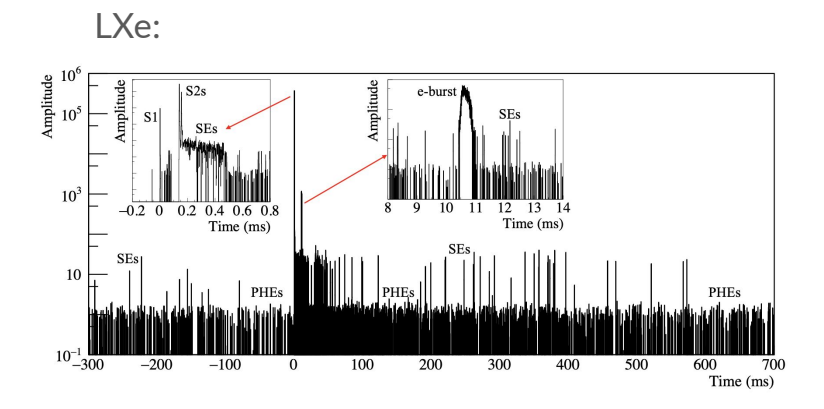
Electroluminescence pulses of unknown origin equivalent to one or few electrons, **correlated** (ms scale) with **preceding events** in the TPC and with **impurities**.

EUV can photo-ionize Xe as well as impurities,

for instance: O₂ (12.1 eV), CH₄ (12.6 eV) and Kr (14.0 eV)

- correlation with preceding events exciting atomic Ar states
- time delays dominated by metastable atomic Ar states



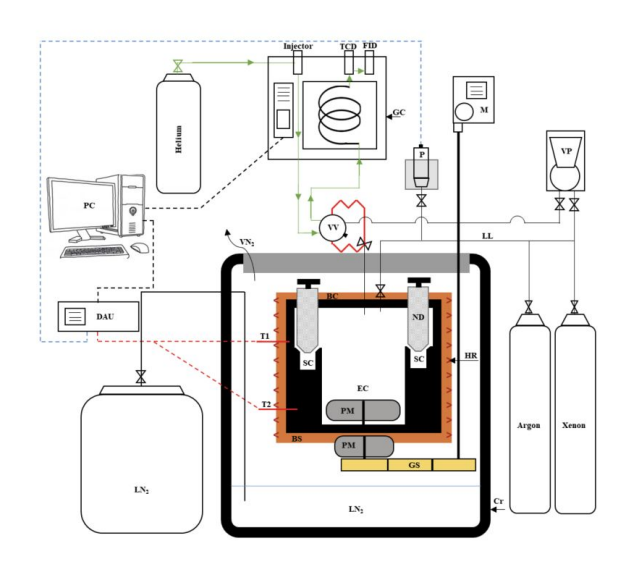


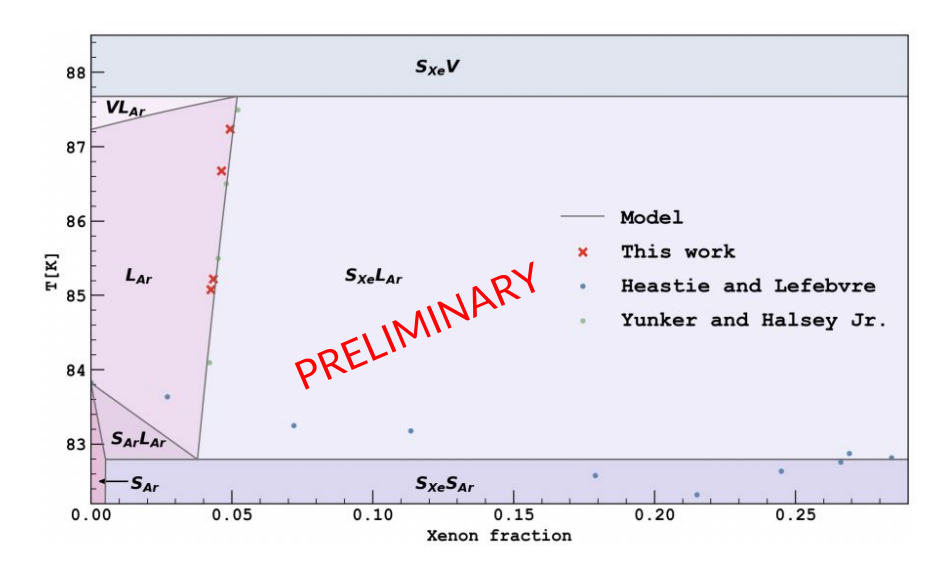
Bonus: first phase-diagram

Study of the solid-vapor and solid-liquid phase equilibrium in the 85-150 K temperature range.

Observations:

- 1. decrease of xenon solubility in the vapor phase with decreasing temperature
- 2. higher but decreasing solubility of xenon in the liquid phase with decreasing temperature: maximum at 4.2%
- 3. measurements in very good agreement with model expectations





Conclusions

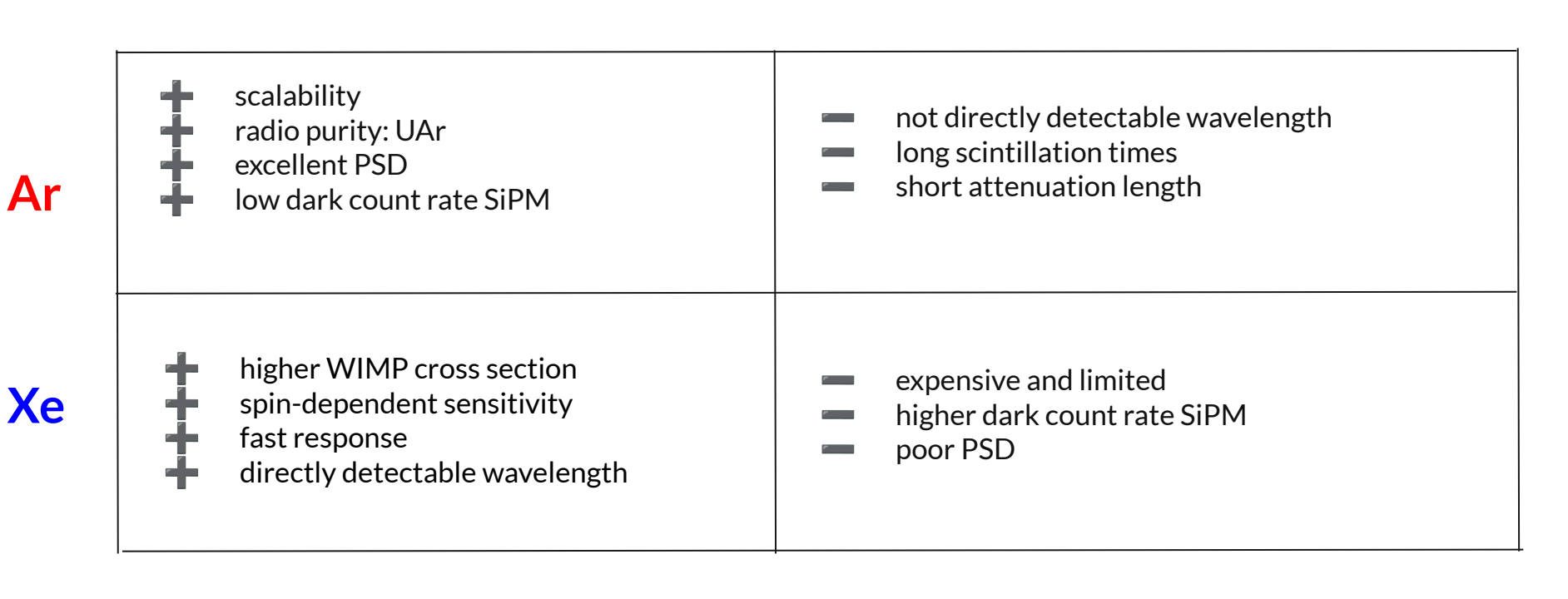
- 1. The **radiative component** addition models <u>pure and xenon-doped</u> liquid argon scintillation.
- 2. In the xenon-doped system we observed an increase in **LY** up to 15 % and a degradation in **PSD** with increasing Xe concentration.
- 3. EUV photon emission can explain the **spurious electrons** in pure LAr, through photoionization of impurities.
- 4. Maximum solubility and phase diagram of the xenon-argon mixture was measured.

Next steps:

- new campaign for investigation of the long component of LAr scintillation
- □ characterization of the ionization response of Xe doped LAr
- thermodynamics paper by the end of the year.

Backup

Argon and xenon as scintillators



SiPM specifications

WW-SiPMs

WL-SiPMs

■ Electrical and optical characteristics

(Typ. T = 25 deg C, Vr = Vop unless otherwise noted)

Parameters	Symbol	Value (typ.)	Unit
Spectral response range	λ	155 to 900	nm
Peak sensitivity wavelength	λр	500	nm
Photon detection efficiency at λp *2	-	32	%
Photon detection efficiency at 175nm	-	24	%
(in vacuum) *2			
Breakdown voltage	V _{br}	53 +/- 5	٧
Recommended operating voltage *3	V _{op}	V _{br} + 4.0	V
Dark count rate / channel	DCR	4.0 (MAX:12)	Mcps
Crosstalk probability	Рст	3	%
Terminal capacitance at Vop / channel	Ct	1200	pF
Gain	М	2.55 x 10 ⁶	-
Temperature coefficient of reverse voltage	ΔTV _{op}	54	mV/deg C
Around room temperature			

^{*2 :} Photon detection efficiency does not include crosstalk and after pulse.

■ Electrical and optical characteristics

(Typ. T = 25 deg C, Vr = Vop unless otherwise noted)

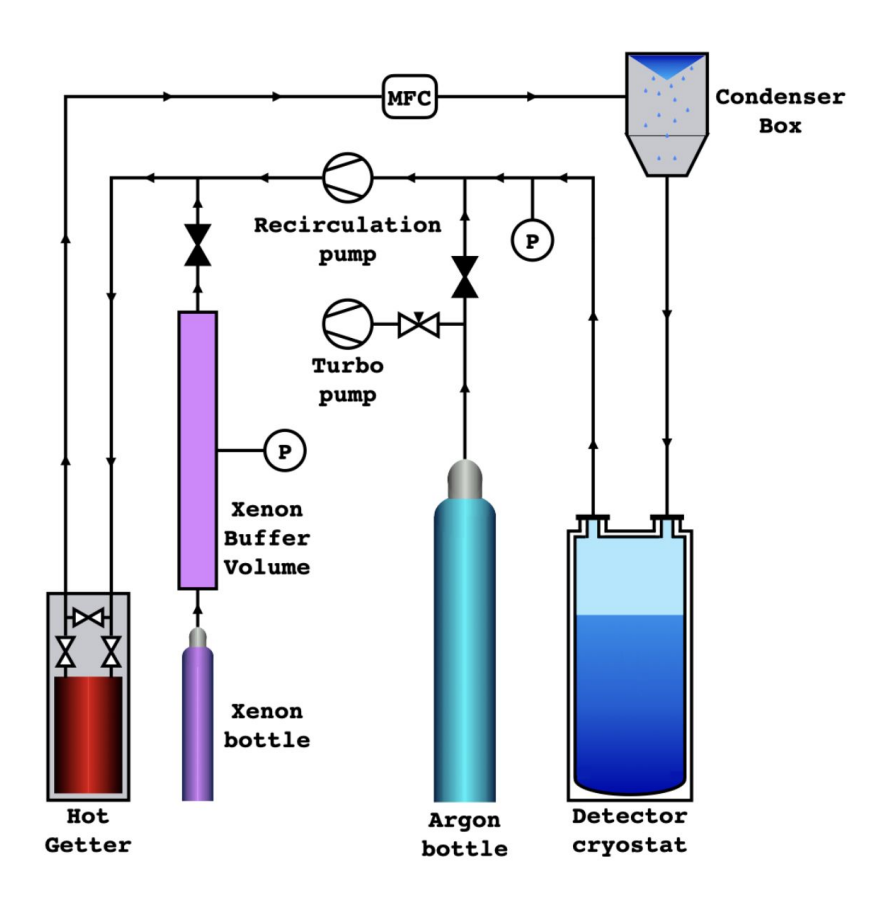
(Typ. 1 = 25 deg C, VI = Vop unless otherwise noted)				
Parameters	Symbol	Value (typ.)	Unit	
Spectral response range	λ	120 to 900	nm	
Peak sensitivity wavelength	λр	500	nm	
Photon detection efficiency at λp *2	•	32	%	
Photon detection efficiency at 175nm (in vacuum) *2	-	24	%	
Breakdown voltage	V _{br}	53 +/- 5	V	
Recommended operating voltage *3	V _{op}	V _{br} + 4.0	V	
Dark count rate / channel	DCR	4.0 (MAX:12)	Mcps	
Crosstalk probability	Рст	3	%	
Terminal capacitance at Vop / channel	Ct	1200	pF	
Gain	М	2.55 x 10 ⁶	-	
Temperature coefficient of reverse voltage Around room temperature	ΔTV _{op}	54	mV/deg C	

^{*2 :} Photon detection efficiency does not include crosstalk and after pulse.

^{*3 :} Refer to the data attached for each products.

^{*3:} Refer to the data attached for each products.

Custom-designed cryogenic system at Princeton



Xe-doped liquid argon scintillation

We fit the waveforms of WW and WL channels simultaneously to disentangle the contributions of components with different wavelengths.

1. Direct Ar scintillation:

$$Ar_2^* \to Ar + Ar + \gamma_{128}$$

2. When Xe is added, ArXe is formed: $Ar_2^* + Xe \rightarrow ArXe^* + Ar$

At ~ 0.2 ppm of Xe:

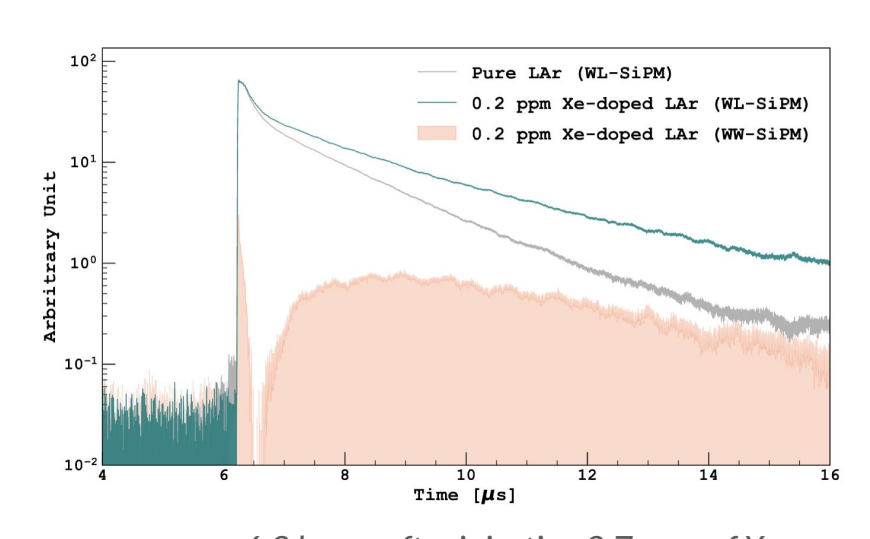
 slow component observed with WL-SiPMs with lifetime ~ 5 ms from ArXe* de-excitation that emits 150 nm photons:

$$ArXe^* \to Ar + Xe + \gamma_{150}$$

At increasing Xe concentration the Xe₂* reaction dominates:

$$ArXe^* + Xe \rightarrow Xe_2^* + Ar$$

Xe₂* decays emitting 175 nm light



6.3 hours after injecting 2.7 ppm of Xe

The Ar-Xe scintillation model

Probability density functions (pdfs) describing the signals observed by the WL and WW channels:

$$f_{WL}(t) = \frac{A}{\varepsilon_{128}} f_{128}(t) + \frac{B_1}{\varepsilon_{150/175}} f_c(t) + \frac{C_1}{\varepsilon_{150/175}} f_r(t)$$

$$f_{WW}(t) = \frac{B_2}{\varepsilon_{150/175}} f_c(t) + \frac{C_2}{\varepsilon_{150/175}} f_r(t)$$

(convoluted with SiPM response)

Amplitudes

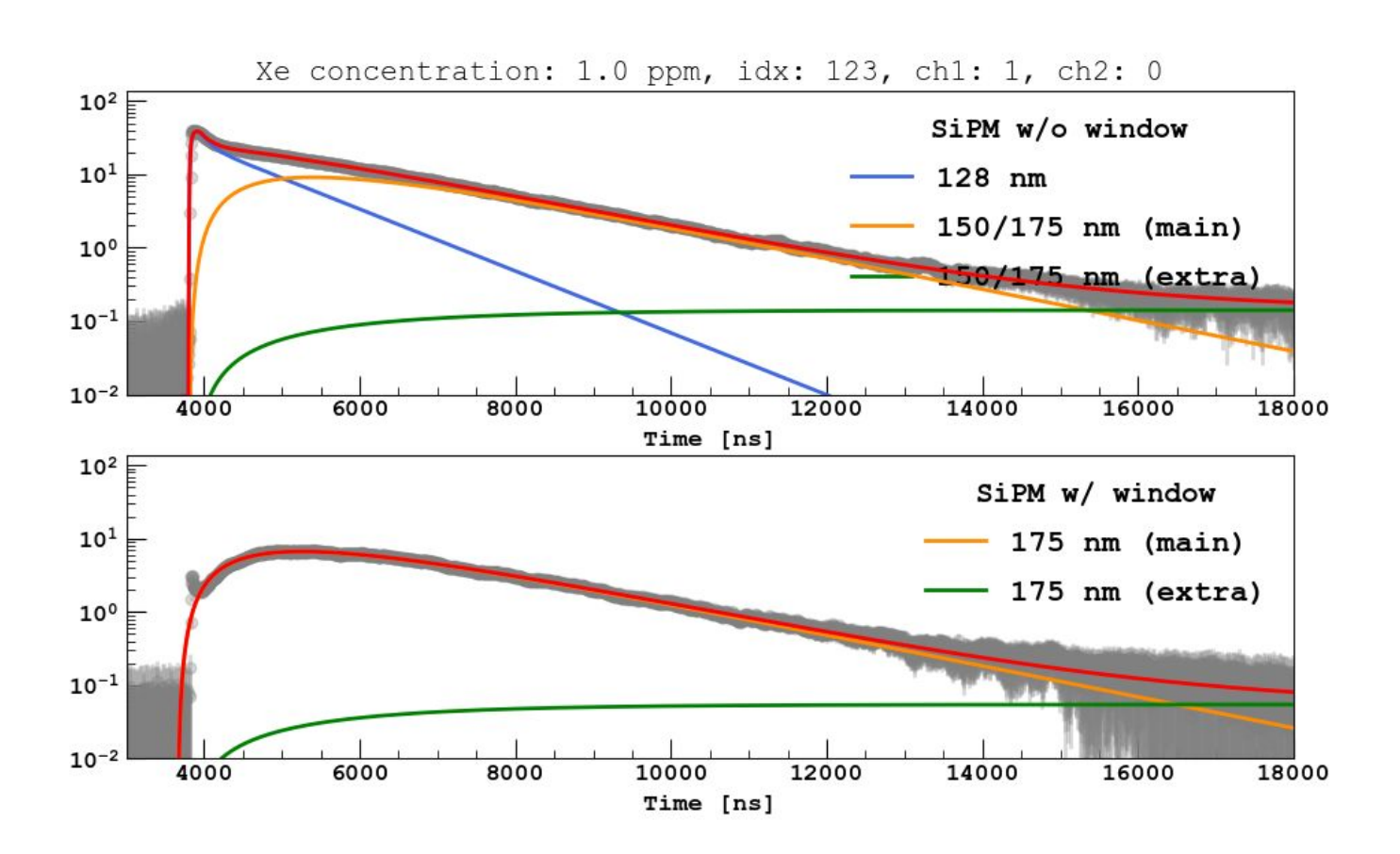
A: Ar₂* de-excitation

B1: collisional component in WL C1: radiative component in WL B2: collisional component in WW

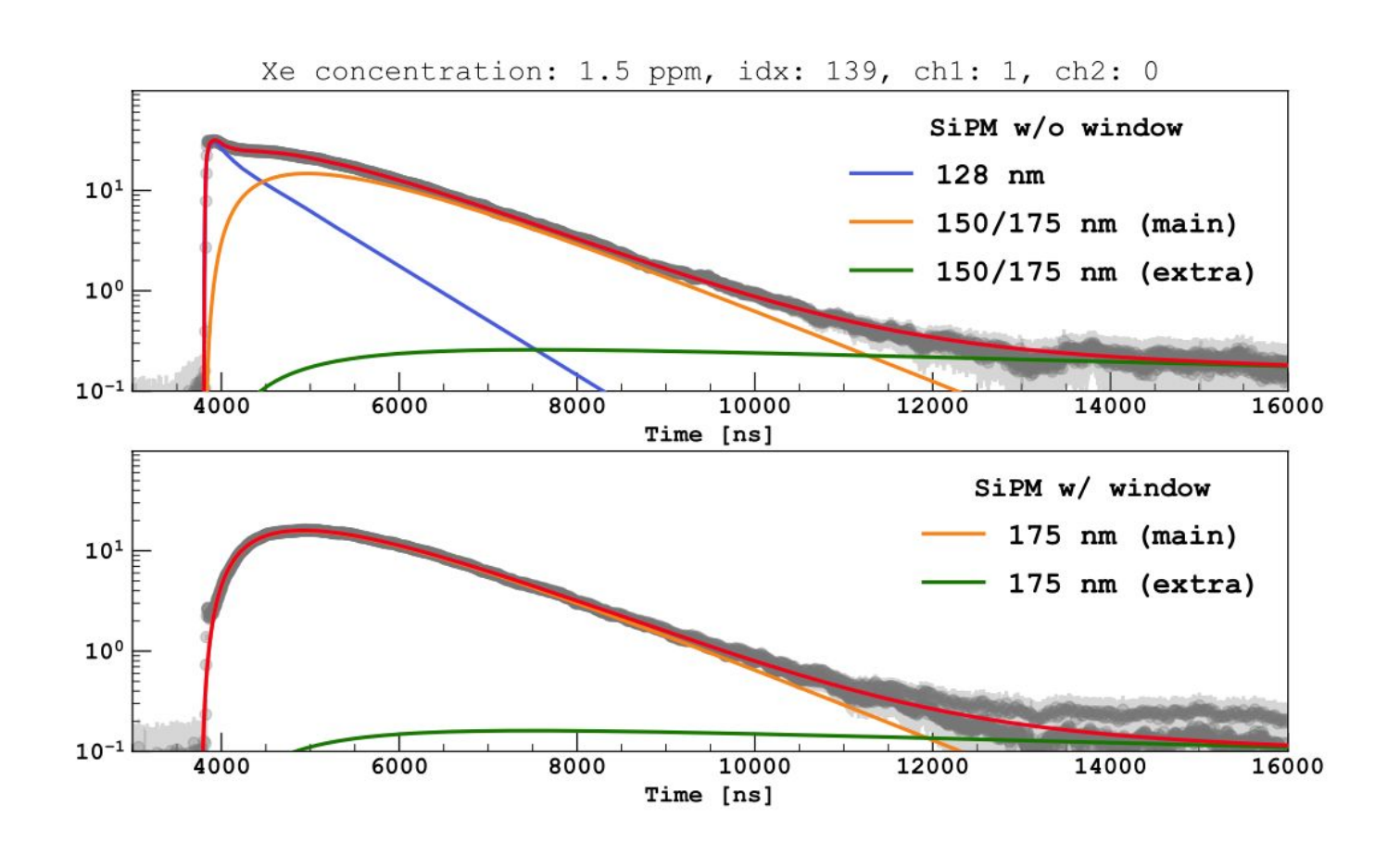
C2: radiative component in WW

E: photodetection efficiencies at different wavelengths

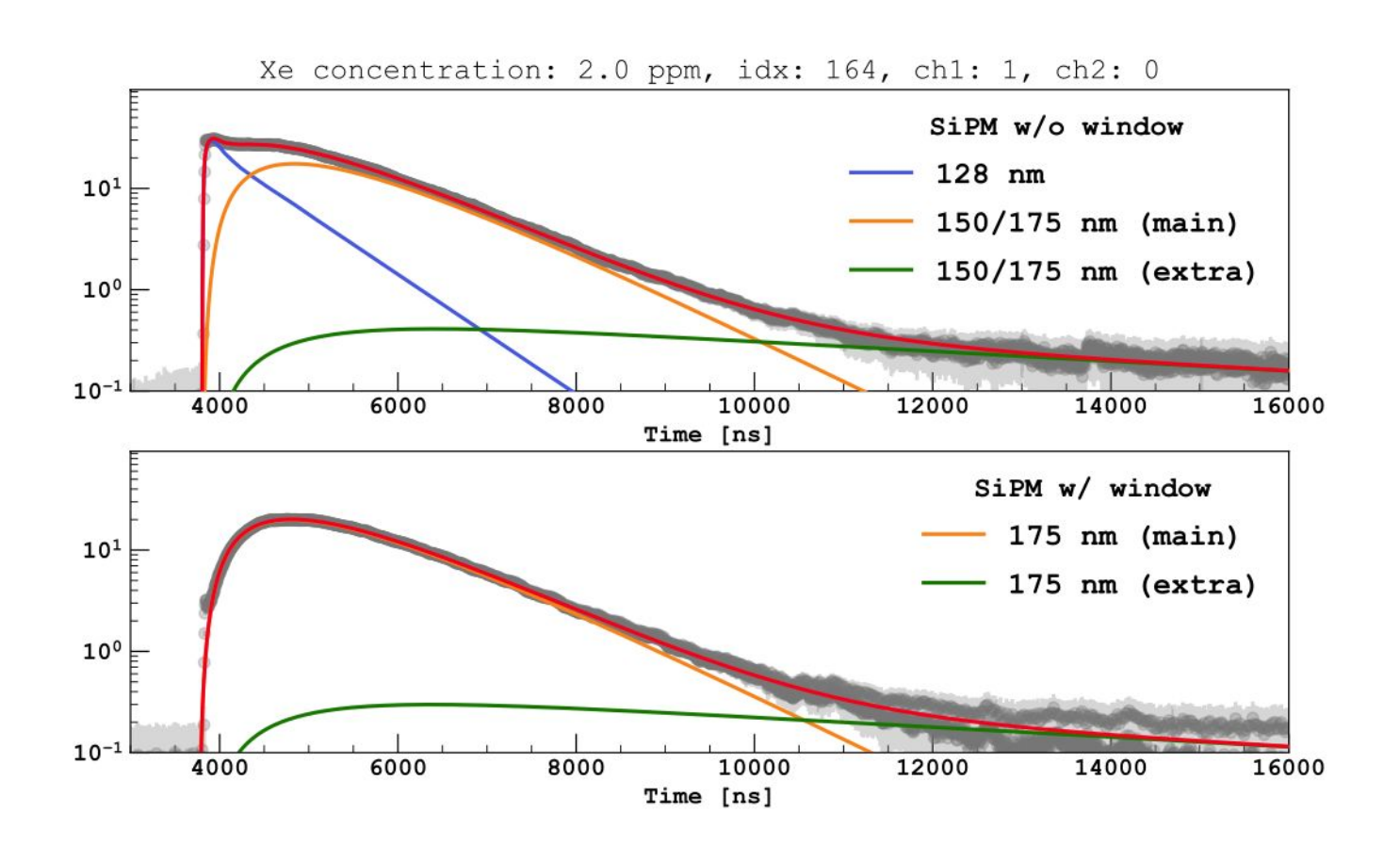
1.0 ppm



1.5 ppm



2.0 ppm



2.7 ppm

